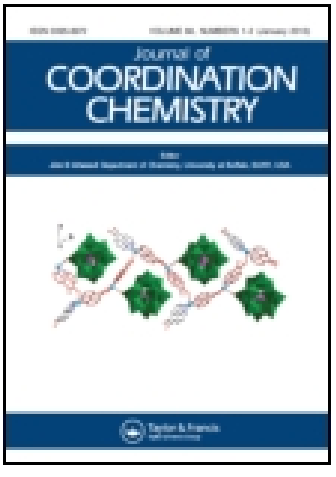

Journal of Coordination Chemistry
Publication details, including instructions for authors and subscription information:
http://www.tandfonline.com/loi/gcoo20

o-Phenylenedioxydiacetate complexes of Gd(III) and Ce(III): syntheses, crystal structures, and magnetic properties

Monika Stolárová[a], Juraj Černák[a], Milagros Tomás[b], Irene Ara[b], Larry R. Falvello[c], Roman Boča[d] & Ján Titiš[d]

[a] Department of Inorganic Chemistry, Faculty of Sciences, P.J. Šafárik University in Košice, Košice, Slovakia

[b] Department of Inorganic Chemistry, Instituto de Síntesis Química y Catálisis Homogénea (ISQCH), University of Zaragoza-CSIC, Zaragoza, Spain

[c] Department of Inorganic Chemistry, Instituto de Ciencia de Materiales de Aragón (ICMA), University of Zaragoza-CSIC, Zaragoza, Spain

[d] Department of Chemistry, FPV, University of SS Cyril and Methodius, Trnava, Slovakia

Accepted author version posted online: 28 Feb 2014.Published online: 03 Apr 2014.

To cite this article: Monika Stolárová, Juraj Černák, Milagros Tomás, Irene Ara, Larry R. Falvello, Roman Boča & Ján Titiš (2014) o-Phenylenedioxydiacetate complexes of Gd(III) and Ce(III): syntheses, crystal structures, and magnetic properties, Journal of Coordination Chemistry, 67:6, 1046-1060, DOI: 10.1080/00958972.2014.898756

To link to this article: http://dx.doi.org/10.1080/00958972.2014.898756

Journal of Coordination Chemistry, 2014
Vol. 67, No. 6, 1046–1060, http://dx.doi.org/10.1080/00958972.2014.898756

o-Phenylenedioxydiacetate complexes of Gd(III) and Ce(III): syntheses, crystal structures, and magnetic properties

MONIKA STOLÁROVÁ†, JURAJ ČERNÁK*†, MILAGROS TOMÁS‡, IRENE ARA‡, LARRY R. FALVELLO*§, ROMAN BOČA¶ and JÁN TITIŠ¶

†Department of Inorganic Chemistry, Faculty of Sciences, P.J. Šafárik University in Košice, Košice, Slovakia
‡Department of Inorganic Chemistry, Instituto de Síntesis Química y Catálisis Homogénea (ISQCH), University of Zaragoza-CSIC, Zaragoza, Spain
§Department of Inorganic Chemistry, Instituto de Ciencia de Materiales de Aragón (ICMA), University of Zaragoza-CSIC, Zaragoza, Spain
¶Department of Chemistry, FPV, University of SS Cyril and Methodius, Trnava, Slovakia

(*Received 3 December 2013; accepted 1 February 2014*)

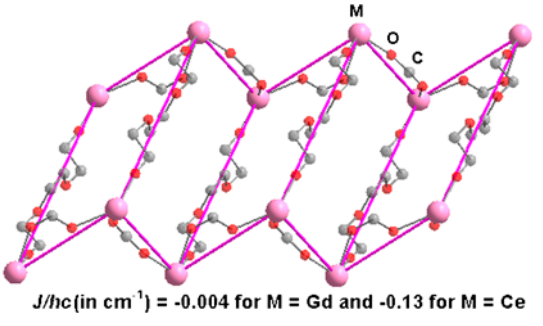

$\{[Ln_2(PDOA)_3(H_2O)_6]\cdot 2H_2O\}_n$ (Ln = Gd, **1**; Ln = Ce, **2**; H_2PDOA = *o*-phenylenedioxydiacetic acid) has been synthesized and characterized by chemical analyses, IR spectroscopy, and thermal analyses. Single-crystal X-ray structure analyses revealed that both **1** and **2** are polymeric and built up of a ladder-like arrangement of Ln(III) ions linked by short *syn-anti* carboxylate bridges and long bridges (legs of the ladder) formed by a second crystallographically independent PDOA. Ln(III) in both **1** and **2** is nine-coordinate with an O_9 donor set formed by one chelating/bridging and one bridging PDOA, and an additional three waters. In the asymmetric unit, there is one crystallographically independent water of crystallization, which is involved in a rich system of hydrogen bonds of the O–H···O type. The identities of the bulk and single crystal phases were corroborated by powder X-ray diffraction. Variable temperature (2–300 K) magnetic studies indicate the presence of only weak antiferromagnetic interactions between pairs of paramagnetic Ln(III) ions with $J/hc = -0.004$ and $-0.13\ cm^{-1}$, for **1** and **2**.

Keywords: Lanthanide; Ligand; X-ray crystal structure; Hydrogen bonding; Magnetic studies

*Corresponding authors. Email: juraj.cernak@upjs.sk (J. Černák); falvello@unizar.es (L.R. Falvello)

1. Introduction

Complexes of lanthanides are studied due to their interesting properties and possible applications [1–4], especially with regard to their magnetic properties [5–10].

Various carboxylates are used in lanthanide complexes [11–15] due to the rich bonding possibilities of carboxylate, which often lead to polymeric structures with various dimensionalities [16–22]. Among organic acids, *o*-phenylenedioxydiacetic acid (H_2PDOA, scheme 1) is, after deprotonation, a versatile multi-dentate chelating/bridging ligand which contains, besides carboxylate, a pair of ether oxygen donors. PDOA can contribute to the formation of secondary structure via the formation of hydrogen bonds and/or π–π stacking interactions [23, 24]. Surprisingly, the potential of this multi-dentate ligand has only scarcely been exploited; few compounds containing PDOA with f-block metals have been reported, e.g. $[Ln_2(PDOA)_3(phen)_2(H_2O)_2]\cdot 2H_2O$ (Ln = Eu, Tb, Dy) (phen = 1,10-phenanthroline), $[La(PDOA)(H_2PDOA)(OH)(H_2O)]\cdot 5H_2O$ [25, 26] and $\{[Ln_2(PDOA)_3(H_2O)_6]\cdot 2H_2O\}_n$ (Ln = Sm, Eu, Dy) [27]. Moreover, luminescence properties of $\{[Gd_2(PDOA)_3(H_2O)_6]\cdot 2H_2O\}_n$ have been studied, and the Gd(III) complex is isostructural with the structurally characterized $\{[Dy_2(PDOA)_3(H_2O)_6]\cdot 2H_2O\}_n$ [28]. As part of our broader study on lanthanide complexes with PDOA [29], here we report our results on the syntheses, crystal structures, and thermal and magnetic properties of $\{[Ln_2(PDOA)_3(H_2O)_6]\cdot 2H_2O\}_n$ [Ln = Gd (**1**), Ce (**2**)].

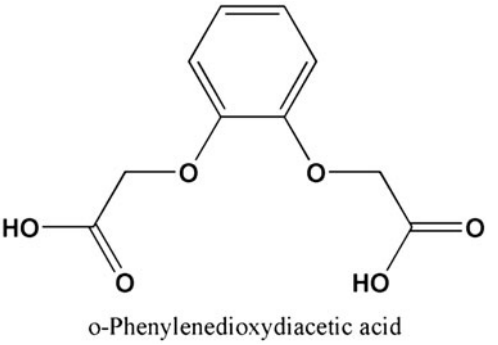

o-Phenylenedioxydiacetic acid

Scheme 1. Structure of H_2PDOA.

2. Experimental

2.1. *Materials*

Gadolinium(III) carbonate hydrate [$Gd_2(CO_3)_3\cdot H_2O$, 99.9%, Aldrich], cerium(III) carbonate hydrate [$Ce_2(CO_3)_3\cdot H_2O$, 99.9%, Aldrich], and *o*-phenylenedioxydiacetic acid (H_2PDOA, $C_{10}H_{10}O_6$, 98%, Aldrich) were purchased.

2.2. *Synthesis of $\{[Ln_2(PDOA)_3(H_2O)_6]\cdot 2H_2O\}_n$ (Ln = Gd, 1; Ln = Ce, 2)*

A mixture of $Ln_2(CO_3)_3\cdot H_2O$ (0.3 mM), H_2PDOA (0.9 mM), and water (10 mL) was placed in a 25 mL Teflon liner, which was heated at 393 K for 30 h and then cooled to room temperature at a rate of 8 °/h. Block crystals of **1** and **2**, insoluble in water and suitable for X-ray structure analyses, were formed. The crystalline product was separated by filtration, followed by washing with distilled water, and finally dried in air. Yields: 56% (**1**); 59% (**2**).

(**1**): Anal. Calcd for $C_{15}H_{20}GdO_{13}$ ($M = 565.56\ g\ M^{-1}$) (%): C, 31.86; H, 3.56. Found: C, 31.70; H, 3.49. IR (cm^{-1}): 3520(w); 3087(w); 1582(s); 1498(s); 1432(s); 1415(m); 1343 (m); 1334(m); 1294(w); 1259(m); 1245(s); 1234(m); 1204(m); 1194(m); 1161(w); 1134(m); 1121(s); 1072(w); 1048(m); 1021(m); 959(m); 920(m); 824(m); 762(m); 750(s); 722(s); 689(m); 598(s); 584(s); 500(m); 468(m); 379(m); 321(m).

(**2**): Anal. Calcd for $C_{15}H_{20}CeO_{13}$ ($M = 548.43\ g\ M^{-1}$) (%): C, 32.85; H, 3.68. Found: C, 32.85; H, 3.94. IR (cm^{-1}): 3183(w); 2933(w); 1592(s); 1501(s); 1457(m); 1433(s); 1419(s); 1406(s); 1343(m); 1333(m); 1295(w); 1259(m); 1250(s); 1236(s); 1198(s); 1194(m); 1169 (w); 1123(s); 1069(w); 1042(m); 1025(s); 958(m); 920(w); 820(m); 765(m); 749(s); 717(s); 694(m); 612(m); 581(s); 524(m); 460(m); 371(w); 320(m).

2.3. *Physical measurements*

CHN analyses were performed on a Perkin Elmer 2400 Series II CHNS/O analyzer. Infrared spectra were recorded on a Perkin Elmer Spectrum 100 CsI DTGS FTIR Spectrometer with UATR 1 bounce-KRS-5 from 4000 to 300 cm^{-1}.

Powder X-ray patterns were taken on a RIGAKU D-Max/2500 diffractometer with rotating anode and RINT2000 vertical goniometer in the range 3°–60° 2θ. The calculated patterns were obtained using the program Mercury CSD 3.1.1 Development.

TG and DTG curves were recorded on a 2960 SDT V3.0 F instrument (aluminum crucibles) in a nitrogen atmosphere from 20 to 250 °C with a heating rate of 5°/min.

2.4. *Magnetic measurements*

The magnetic data were measured using a SQUID apparatus (MPMS-XL7, Quantum Design) using the RSO mode of detection with ca. 25 mg of the sample encapsulated in a gelatin-made sample holder. The molar susceptibility χ_M taken at $B = 0.1\ T$ was corrected for the underlying diamagnetism and converted to the effective magnetic moment μ_{eff}. The magnetization M_M was measured at two temperatures: $T = 2.0$ and 4.6 K.

2.5. *X-ray experiment*

Collection of single-crystal X-ray data was performed on a Bruker CCD-based four-circle diffractometer at 100(1) K (**1**) and on an Oxford Diffraction Xcalibur diffractometer equipped with a Sapphire3 CCD detector at 173(1) K (**2**). Both diffractometers were equipped with a graphite monochromator utilizing MoKα radiation ($\lambda = 0.71073$ Å). Absorption corrections based on the multi-scan method using SADABS were applied for **1** [30], while data for **2** were corrected based on the multi-scan technique using CrysAlis [31]. The structures were solved by SIR92 [32] and refined against the F^2 data using full-matrix least squares methods with the program SHELXL-97 [33]. Anisotropic displacement parameters were refined for all non-H atoms. Hydrogens bonded to carbon and oxygen were included at idealized positions and refined as riders with isotropic displacement parameters assigned as 1.2 times the U_{eq} values of the corresponding bonding partners. The crystal and experimental data are given in table 1 and the selected geometric parameters are given in table 2. Possible hydrogen bonds are gathered in tables 3 and 4. The structural figures were drawn using Diamond [34].

Table 1. Crystal data and structure refinements for **1** and **2**.

	1	**2**
Empirical formula	$C_{15}H_{20}GdO_{13}$	$C_{15}H_{20}CeO_{13}$
Molecular weight	565.56	548.43
Crystal system	Orthorhombic	Monoclinic
Space group	*Pbcn*	*C2/c*
Unit-cell dimensions		
a (Å)	34.1184 (15)	34.1989 (8)
b (Å)	12.5956 (5)	12.4413 (2)
c (Å)	8.3102 (4)	8.8330 (2)
β (°)	90	91.210 (2)
V (Å^3)	3571.2 (5)	3757.39 (14)
Z	8	8
D_{Calcd} (Mg m^{-3})	2.104	1.939
T (K)	100 (1)	173 (1)
μ (mm^{-1})	3.787	2.495
Crystal dimensions (mm)	0.146 × 0.093 × 0.066	0.25 × 0.18 × 0.04
Crystal color/form	Colorless/plate	Colorless/plate
Index ranges	$-43 \le h \le 43$	$-47 \le h \le 48$
	$-15 \le k \le 16$	$-16 \le k \le 17$
	$-6 \le l \le 10$	$-12 \le l \le 12$
θ Ranges (°)	1.72–26.95	1.74–28.64
Reflections collected	3884	5422
Independent reflections	3517 ($R_{int} = 0.0328$)	4747 ($R_{int} = 0.0322$)
Absorption corr. method	Multi-scan	Multi-scan
T_{min} T_{max}	0.8015–1.0000	0.7348–1.0000
Goodness-of-fit on F^2	1.080	1.048
R indices [$I > 2\sigma(I)$]	$R_1 = 0.0215$, $wR_2 = 0.0486$	$R_1 = 0.0237$, $wR_2 = 0.0468$
R indices (all data)	$R_1 = 0.0252$, $wR_2 = 0.0501$	$R_1 = 0.0301$, $wR_2 = 0.0504$
Diff. peak and hole (e Å^{-3})	0.733; −0.939	1.063; −0.589

Table 2. Selected geometric parameters [Å, °] for **1** and **2**.

	1	**2**		**1**	**2**
Ln1–O1	2.415 (2)	2.473 (2)	O7–C11	1.267 (3)	1.252 (3)
Ln1–O2	2.412 (2)	2.482 (2)	O8–C11	1.237 (3)	1.236 (3)
Ln1–O3	2.562 (2)	2.636 (2)	O1–Ln1–O3	61.84 (6)	91.41 (10)
Ln1–O4	2.642 (2)	2.703 (2)	O3–Ln1–O4	59.28 (5)	58.63 (4)
Ln1–O5	2.401 (2)	2.472 (2)	O4–Ln1–O5	62.68 (5)	60.34 (5)
Ln1–O7	2.297 (2)	2.380 (2)	O5–Ln1–O7	90.66 (6)	86.12 (6)
Ln1–O10w	2.351 (2)	2.516 (2)	O5–Ln1–O2^{i}	142.26 (2)	143.51 (2)
Ln1–O11w	2.434 (3)	2.560 (2)	O7–Ln1–O11w	82.29 (7)	80.95 (6)
Ln1–O12w	2.507 (3)	2.517 (2)	O5–C10–O6	125.76 (2)	124.87 (2)
O5–C10	1.265 (3)	1.265 (2)	Ln1–O7–C11	169.66 (2)	172.42 (2)
O6–C10	1.252 (3)	1.244 (3)			

Note: Symmetry code: (i) x, $1 - y$, $z - 1/2$.

3. Results and discussion

3.1. *Synthesis, identification, and thermal study of dehydration*

From the aqueous systems Ln(III) – H_2PDOA (Ln = Ce, Gd) using hydrothermal conditions **1** and **2**, $\{[Ln_2(PDOA)_3(H_2O)_6]\cdot 2H_2O\}_n$, were formed in the form of single crystals suitable for X-ray data collection. The results of chemical analyses corroborated the fact that the composition of **1** and **2** corresponds to that of previously characterized analogous complexes with Ln = Sm, Eu, and Dy [27–29]. The phase purity and identity of the samples

Table 3. Possible hydrogen bonds for **1** [Å and °].

D–H…A	*d*(D–H)	*d*(H…A)	*d*(D…A)	∠(DHA)
O(10W)–H(10C)…O(6)^{iv}	0.81 (5)	1.88 (5)	2.689 (3)	174 (4)
O(10W)–H(10D)…O(6)^{v}	0.75 (4)	2.09 (4)	2.810 (3)	162 (4)
O(11W)–H(11C)…O(1)^{i}	0.81 (4)	1.94 (4)	2.721 (3)	162 (4)
O(11W)–H(11D)…O(13W)	0.81 (4)	1.86 (4)	2.648 (3)	167 (4)
O(12W)–H(12C)…O(5)^{iv}	0.79 (4)	2.11 (4)	2.891 (3)	169 (3)
O(12W)–H(12D)…O(6)^{vi}	0.74 (3)	2.50 (3)	3.194 (3)	157 (4)
O(12W)–H(12D)…O(11W)^{iv}	0.74 (3)	2.58 (4)	2.994 (3)	117 (3)
O(13W)–H(13D)…O(12W)^{vii}	0.73 (5)	2.18 (5)	2.874 (3)	160 (5)
O(13W)–H(13C)…O(8)	0.98 (5)	1.71 (5)	2.681 (3)	173 (4)

Note: Symmetry codes: (i) x, $1-y$, $z-1/2$; (iv) $3/2-x$, $3/2-y$, $z+1/2$; (v) $3/2-x$, $y-1/2$, z; (vi) x, $2-y$, $z+1/2$; (vii) x, y, $z-1$.

Table 4. Possible hydrogen bonds for **2** [Å and °].

D–H…A	*d*(D–H)	*d*(H…A)	*d*(D…A)	∠(DHA)
O(10W)–H(10C)…O(13w)^{viii}	0.74 (3)	2.29 (3)	2.978 (3)	154 (4)
O(10W)–H(10D)…O(6)^{viii}	0.87 (3)	1.84 (3)	2.706 (2)	177 (3)
O(10W)–H(10D)…O(5)^{viii}	0.84 (3)	1.92 (3)	2.760 (2)	177 (3)
O(11W)–H(11C)…O(1)^{i}	0.81 (3)	1.92 (3)	2.699 (2)	160 (3)
O(12W)–H(12C)…O(13w)^{ix}	0.79 (3)	1.95 (3)	2.723 (3)	164 (3)
O(12W)–H(12D)…O(6)^{vi}	0.81 (3)	2.00 (3)	2.800 (2)	171 (3)
O(13W)–H(13D)…O(11W)	0.80 (4)	2.03 (4)	2.821 (3)	170 (4)
O(13W)–H(13C)…O(8)	0.81 (4)	1.95 (4)	2.752 (3)	173 (4)

Note: Symmetry codes: (i) x, $1-y$, $z-1/2$; (vi) x, $2-y$, $z+1/2$; (viii) $3/2-x$, $3/2-y$, $1-z$; (ix) x, y, $z+1$.

were checked by powder X-ray diffraction (figure S1, see online supplemental material at http://dx.doi.org/10.1080/00958972.2014.898756). It should be noted that complex **1** (Ln = Gd) was previously mentioned in the literature, but that product was prepared from aqueous solution using the perchlorate salt of Gd(III) and H_2PDOA [28].

In order to estimate the water content and to follow the dehydration in **1** (figure S2) and **2** (figure 1), their TG and DTA curves up to 250 °C were recorded. The dehydration processes in **1** and **2** are analogous, so they will be discussed simultaneously and the data from **2** will be given in parentheses. The dehydration of **1** is observed from 51 to 170 °C (47–195 °C for **2**), and the observed weight loss is 12.7% (13.6%). This value corresponds well to the calculated value of 12.7% (13.1%) for complete dehydration. In the analogous complex with Ln = Dy, the dehydration occurred from 73 to 149 °C, indicating its higher thermal stability [27]. As indicated by the DTA curves, the dehydrations of both **1** and **2** are endothermic multi-step processes.

In the case of **2**, the dehydration was also followed by IR spectroscopy. As can be seen from figure 1, in the IR spectrum of the dehydrated sample **2a** prepared by static heating at 160 °C for 30 min, the absorption bands arising from ν(OH) stretching and $\delta(H_2O)$ deformation are missing.

3.2. *IR spectra*

IR spectra of **1** and **2** (figure S3) are dominated by the PDOA ligand, so the identification and tentative assignment of the observed absorptions to the individual vibration types was only partially possible. Several weak absorptions positioned below 3000 cm^{-1} in both **1** and **2** can be attributed to ν(CH) of the methylene groups. Weak bands above 3000 cm^{-1} may

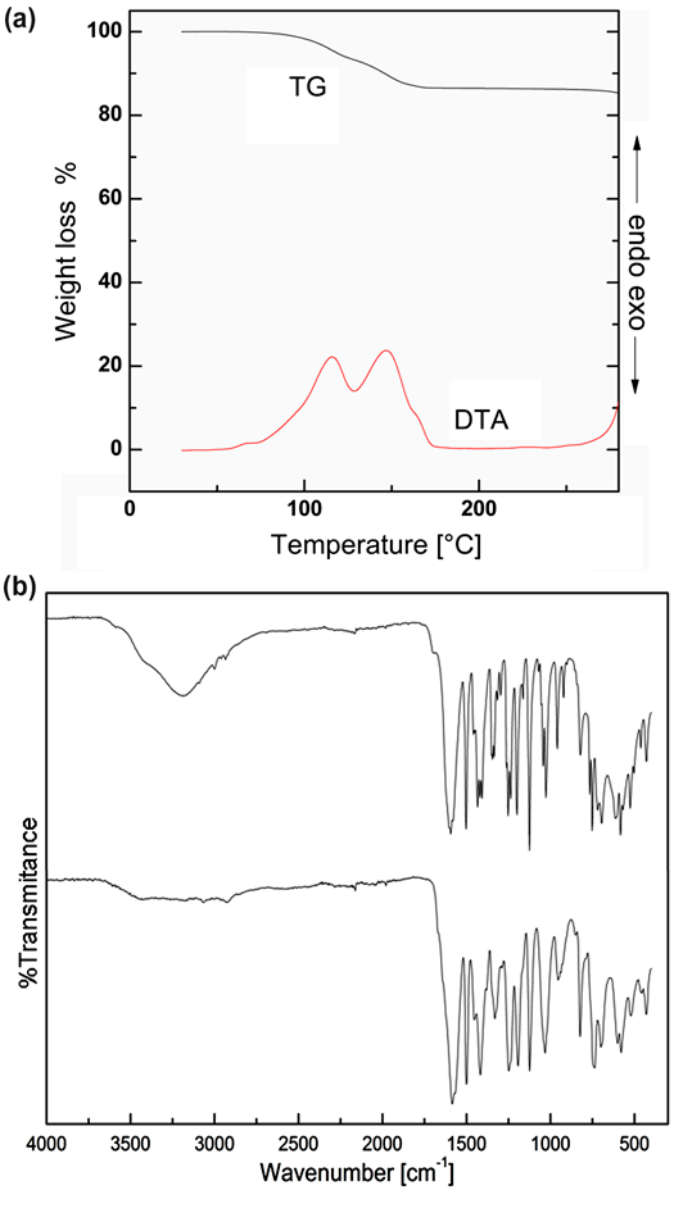

Figure 1. TG and DTA curves for **2** (a); IR spectra of **2** (room temperature; above) and **2a** (previously heated at 160 °C; below) (b).

arise from the ν(CH) of the aromatic rings. The presence of water manifests itself by a rather sharp ν(OH) absorption at 3520 cm^{-1} in **1** and further broad absorptions centered around 3300 cm^{-1}. While the weak peak at 3520 cm^{-1} can be assigned to ν(OH) of the O9–H9WB, which is apparently not involved in hydrogen bond (HB) formation, the remaining water hydrogens are involved in HBs which shift their absorption to lower wavenumbers. The corresponding deformation vibration $\delta(OH_2)$ can be found as a weak shoulder

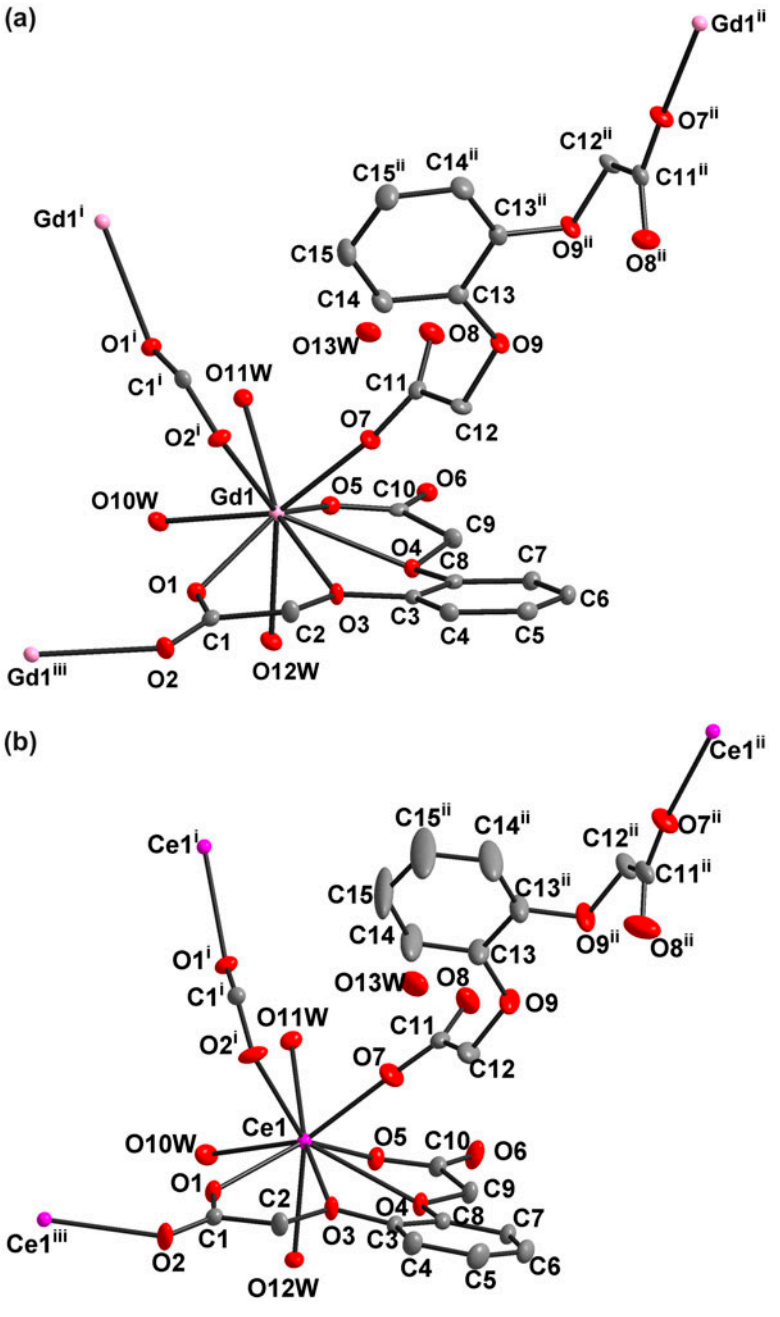

Figure 2. The coordination modes of the Gd(III) and Ce(III) atoms in **1** (a) and **2** (b). The thermal ellipsoids are drawn at the 50% probability level. Hydrogen atoms are omitted for the sake of clarity.
Note: Symmetry codes: (i) x, $1-y$, $z-1/2$; (ii) $1-x$, y, $1/2-z$; (iii) x, $1-y$, $1/2+z$.

at 1673 cm^{-1} in **1**. In the spectrum of **2** a typical broad, medium-intensity absorption for hydrogen bonded water is centered around 3183 cm^{-1}, accompanied by a weak shoulder at 3500 cm^{-1}. The corresponding deformation vibration $\delta(OH_2)$ can be found as a weak shoulder at 1694 cm^{-1}.

Absorption bands due to asymmetric and symmetric ν(COO) vibrations of the carboxylates can be found in the spectrum of **1** at 1582 cm^{-1} (1592 cm^{-1} for **2**) and 1432 cm^{-1} (1433 cm^{-1} for **2**), respectively. The presence of the aromatic rings can be deduced from the sharp absorptions at 1498 cm^{-1} (1501 cm^{-1} for **2**); this band can be found at 1505 cm^{-1} in the spectrum of H_2PDOA.

3.3. *Crystal structures*

The crystal structures of both compounds $\{[Ln_2(PDOA)_3(H_2O)_6]\cdot 2H_2O\}_n$ (Ln = Gd for **1** and Ce for **2**) (figure 2) are formed by a staircase- or ladder-like arrangement of Gd(III) and Ce(III), respectively (figures 3 and S3). The same type of ladder-like structure was already described for analogous compounds with Ln = Sm, Eu and Dy [27–29]: the ladders are built up of two $[–Ln–O–C–O–]_n$ zigzag chains interlinked by bidentate PDOA. Within the chains running along the *c* axis Ln(III) ions are linked by *syn-anti* carboxylate bridges. The resulting arrangement topologically recalls the β-sheet secondary structure of the proteins (figure 3). The shortest Ln···Ln distances are found within a given chain [6.149(3) Å for Gd···Gd in **1** and 6.332(2) Å for Ce···Ce in **2**]; the inter-chain Ln(III) contacts are longer [13.987(5) Å in **1** and 14.219(4) Å in **2**]. These values are comparable with the corresponding distances of 6.276(5) and 14.128(5) Å observed in $\{[Sm_2(PDOA)_3(H_2O)_6]\cdot 2H_2O\}_n$ [27].

The central Ln(III) in both **1** and **2**, as in the previously studied compounds with Dy, Sm, and Eu [27], exhibit nine-coordination with an $O_4O_3O_2$ donor set; the polyhedron can be described as a deformed triply capped trigonal prism (figure 4). Four oxygens (O1, O3, O4, and O5) originate from the chelate of the pentadentate PDOA (the fifth oxygen is used for *syn-anti* bridging) and a further two oxygens (O2 and O7) are from two crystallographically different PDOA ligands, both linking Ln(III) ions: O2 is from the PDOA which links neighboring Ln(III) ions via a *syn-anti* bridging carboxylate. O7 belongs to the bridging

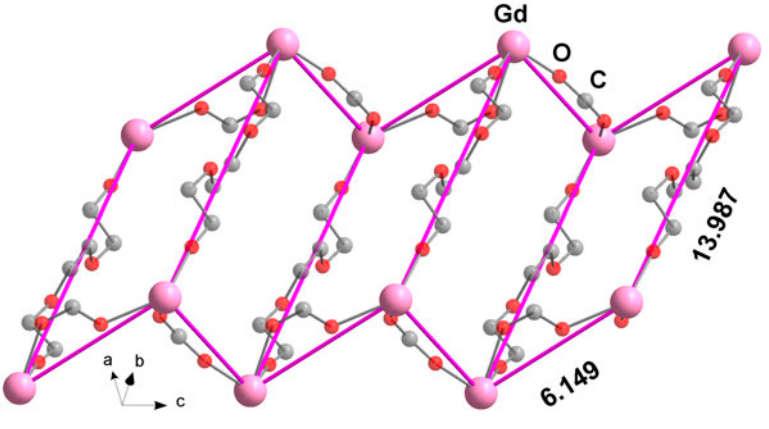

Figure 3. Ladder-like arrangement of Gd(III) atoms in **1** linked by short *syn-anti* carboxylate bridges and long bridges through the PDOA ligands. Only atoms forming the bridges are shown.

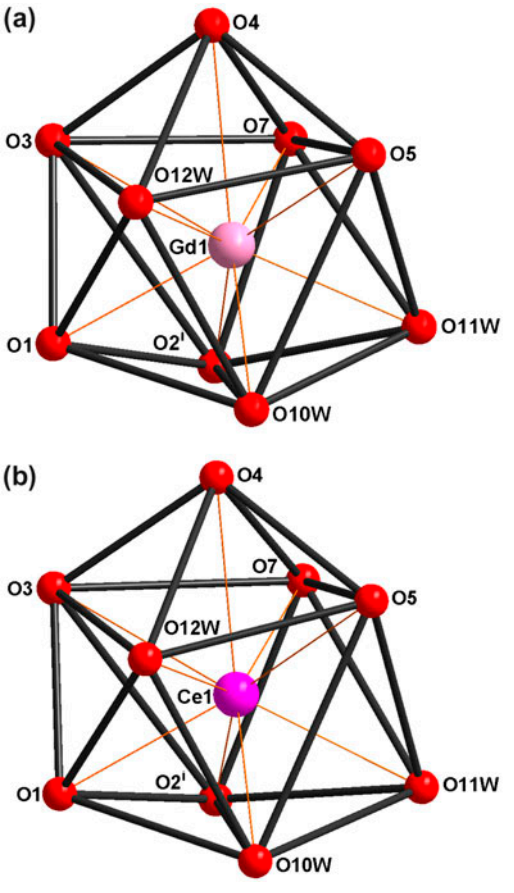

Figure 4. Coordination polyhedra of the Gd1 (a) and Ce1 atoms (b) in **1** and **2**, respectively.
Note: Symmetry code: (i) x, $1-y$, $z-1/2$.

bidentate PDOA which exhibits twofold internal symmetry. Additionally, Ln(III) is coordinated by three waters (O10w, O11w, and O12w).

The Gd–O bonds are 2.351(2)−2.642(2) Å with the longest bonds of 2.562(2) and 2.642 (2) Å formed by O3 and O4 phenolate, suggesting their weaker coordination (table 2). In $[Gd_2(H_2bta)(bta)(H_2O)_2]_n \cdot 4nH_2O$ (H_4bta = 1,2,4,5-benzenetetracarboxylic acid), in which only carboxylate and water oxygens coordinate to Gd(III), the Gd–O distances were 2.3433 (19)−2.5731(18) Å [35]. The corresponding Ce–O distances in **2** are 2.3802(17)−2.7032 (14) Å (table 2); the largest Ce–O distances [2.6357(16) and 2.7032(14) Å] are formed with the phenolato oxygens. A similar range of Ce–O bonds [2.390(3)−2.698(3) Å] was observed in $[Ce(Hcit)(H_2O)]_n$ (H_4cit = citric acid) [36].

Compounds **1** and **2** exhibit different packing of the neighboring ladders (figure S4), reflected in the different crystal systems and space groups of the two structures – **1** is orthorhombic (*Pbcn*) and **2** is monoclinic (*C2/c*). A similar situation, as noted [27], was observed for analogous compounds with Dy(III) (*Pbcn*), Sm (*C2/c*), and Eu (*C2/c*); compounds crystallizing in the same space group are isostructural. The analogous Eu(III) complex,

$[Eu_2(PDOA)_3(H_2O)_6]\cdot 2H_2O$, was described in both orthorhombic [28] and monoclinic [27] forms; as the respective diffraction data were collected at laboratory (296 K, monoclinic, *C2/c*) and low (100 K, orthorhombic, *Pbcn*) temperatures, it was not immediately clear if the observed polymorphism is a manifestation of a phase transition or whether both phases can coexist. We measured the cell parameters of **1** and **2** at room temperature; both compounds retain their symmetries and cell dimensions at both room temperature and low temperature, which provides experimental confirmation that there is no phase transition. A closer look at the structures (figure S5) reveals packing arrangements that would require major structural reorganization in order to produce a phase transition from one to the other.

An interesting point which should be mentioned concerns the unusually large and prolate displacement surfaces of the phenyl carbons of the bidentate bridging PDOA in **2**. As can be seen in figure 5(a), the displacement ellipsoids of the carbons forming the phenyl group of the bridging PDOA ligand in **1** display normal values. In **2**, the analogous carbons exhibit rather high displacement [figure 5(b)]. In **1**, the distance between the centroids (Cg1) of the neighboring aromatic rings is 4.486(2) Å while the perpendicular distance between aromatic rings is 3.2529(12) Å, suggesting weak π–π interaction. On the other hand, in **2** the corresponding distance between the centroids is longer, 4.713(3) Å, and the perpendicular distance is 3.6986(19) Å. These observations suggest that the high thermal motion of the carbons can be interpreted as an approach of the aromatic rings to each other in order to

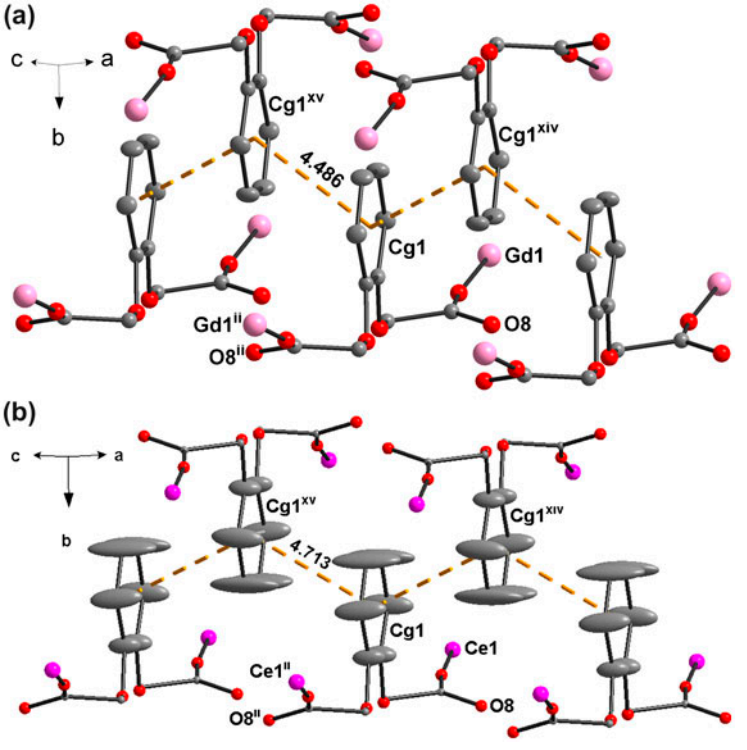

Figure 5. Weak π–π interactions and large thermal motion of the phenyl group carbon atoms in **1** (a) and **2** (b).
Note: Symmetry codes: (xiv) $1-x, 1-y, -z$; (xv) $1-x, 1-y, 1-z$.

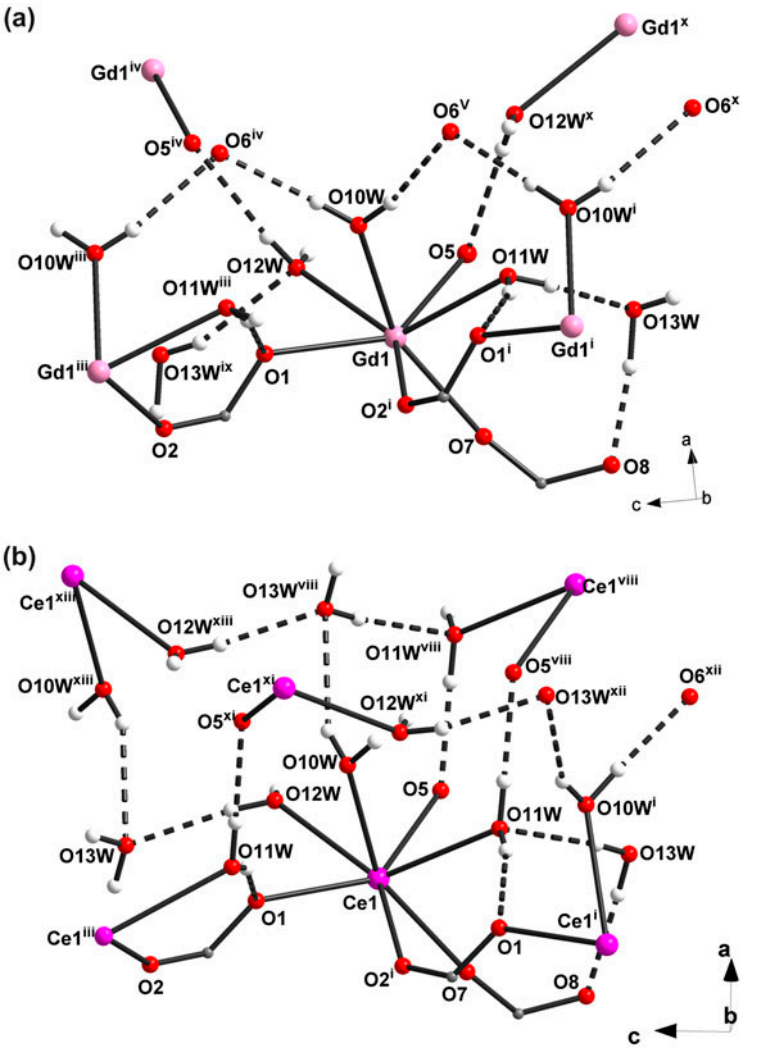

Figure 6. Hydrogen bonding systems in **1** (a) and **2** (b).
Note: Symmetry codes: (x) $3/2 - x$, $3/2 - y$, $z - 1/2$; (xi) $3/2 - x$, $y - 1/2$, $3/2 - z$; (xii) $3/2 - x$, $y - 1/2$, $1/2 - z$; (xiii) $3/2 - x$, $3/2 - y$, $2 - z$.

maximize the attractive interaction; the observed data do not allow us to distinguish between a static and dynamic model of the observed disorder.

The crystal structures of both **1** and **2** are additionally stabilized by hydrogen bonds of the O–H···O type from carboxylate oxygens, coordinated water, and the one crystallographically independent solvate water (O13w) (figure 6, table 3).

3.4. *Magnetic properties*

Gd(III) possesses the ground electronic term ^8S that is orbitally non-degenerate and well separated from the excited terms. For this reason, the magnetogyric factor stays $g \sim 2$. The

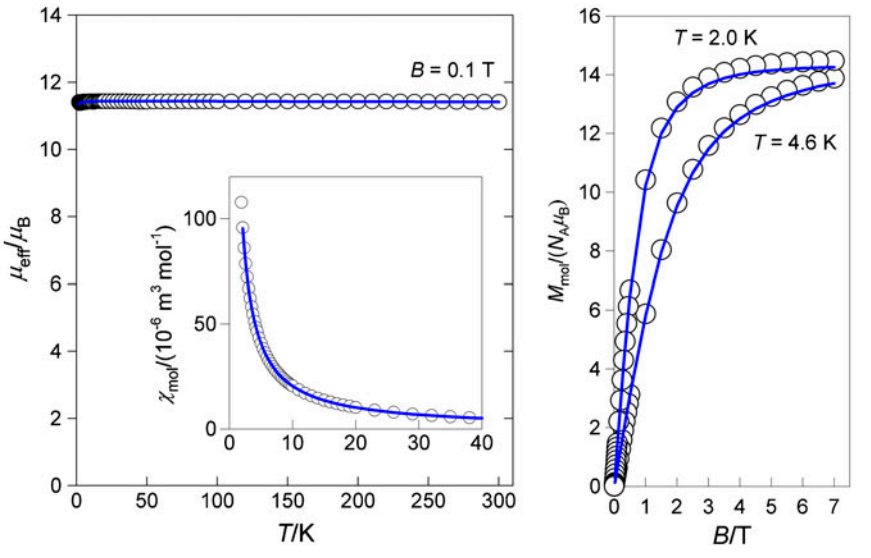

Figure 7. Magnetic functions for **1**. Left – temperature dependence of the effective magnetic moment, right – field dependence of the magnetization, inset – temperature dependence of the molar magnetic susceptibility. Open circles – experimental data; lines – fitted.

high-temperature limit of the effective magnetic moment for a single Gd(III) with spin $s = 7/2$ and $g = 2$ is $\mu_{\mathrm{eff}}(\mathrm{Gd}) = g[s(s+1)]^{1/2} = 7.94\ \mu_{\mathrm{B}}$; for a pair of them it is $\mu_{\mathrm{eff}}(2\mathrm{Gd}) = 11.2\ \mu_{\mathrm{B}}$. Dealing with the formula unit $C_{30}H_{40}O_{24}Gd_2 \cdot 2(H_2O)$ and $M = 1131.12\ \mathrm{g\,M^{-1}}$ the magnetic data for **1** are displayed in figure 7. The effective magnetic moment at room temperature adopts the value of $\mu_{\mathrm{eff}} = 11.4\ \mu_{\mathrm{B}}$ and stays nearly constant down to $T = 1.9$ K. The magnetic susceptibility increases monotonously on cooling, confirming that the Curie law is obeyed almost perfectly. The magnetization per formula unit saturates at $B = 7$ T and $T = 2.0$ K to the value of $M_1 = M_{\mathrm{M}}/N_{\mathrm{A}}\mu_{\mathrm{B}} = 14.5$ that is close to the spin-only value (14.0 for the dinuclear unit).

The fitting procedure applied to both data-sets (temperature dependence of the susceptibility and field dependence of the magnetization) gave the following set of magnetic parameters: isotropic exchange coupling constant $J/hc = -0.0040\ \mathrm{cm^{-1}}$, $g = 2.042$, and the temperature-independent term $\chi_{\mathrm{TIM}} = -4.0 \times 10^{-9}\ \mathrm{m^3\,M^{-1}}$. The last term compensates the uncertainties in the estimates of the underlying diamagnetism and reflects a diamagnetic signal of the sample holder. The discrepancy factor for the susceptibility and magnetization are $R(\chi) = 0.0037$ and $R(M) = 0.014$, respectively. The very small value of the exchange coupling constant confirms that the paramagnetic centers are almost uncoupled.

The magnetic data for the Ce(III) complex, **2**, are in many respects different (figure 8). The effective magnetic moment gradually decreases from its room temperature value of $\mu_{\mathrm{eff}} = 3.25\ \mu_{\mathrm{B}}$ to the value of $\mu_{\mathrm{eff}} = 2.54\ \mu_{\mathrm{B}}$ at $T = 1.9$ K. The spin-only value for two uncoupled $s = 1/2$ centers is $\mu_{\mathrm{eff}} = g[2s(s+1)]^{1/2} = 2.25\ \mu_{\mathrm{B}}$. The magnetization per formula unit saturates at $B = 7$ T and $T = 2.0$ K to the value of $M_1 = M_{\mathrm{M}}/N_{\mathrm{A}}\mu_{\mathrm{B}} = 2.46$ that is higher relative to the spin-only value (2.0 for the dinuclear unit composed of $s = 1/2$ spins). These features confirm that some orbital contribution raises the g-factor and, in addition, close-lying excited states exist.

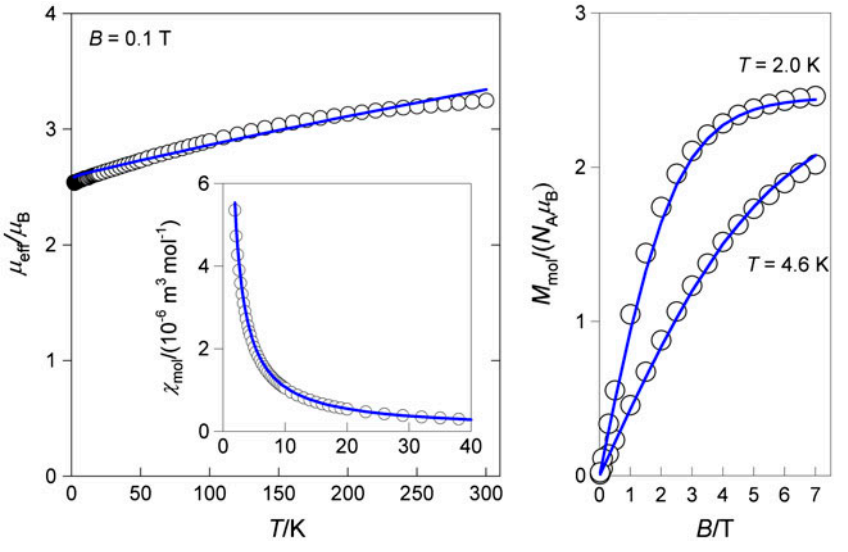

Figure 8. Magnetic functions for **2**. Left – temperature dependence of the effective magnetic moment, right – field dependence of the magnetization, inset – temperature dependence of the molar magnetic susceptibility. Open circles – experimental data; lines – fitted.

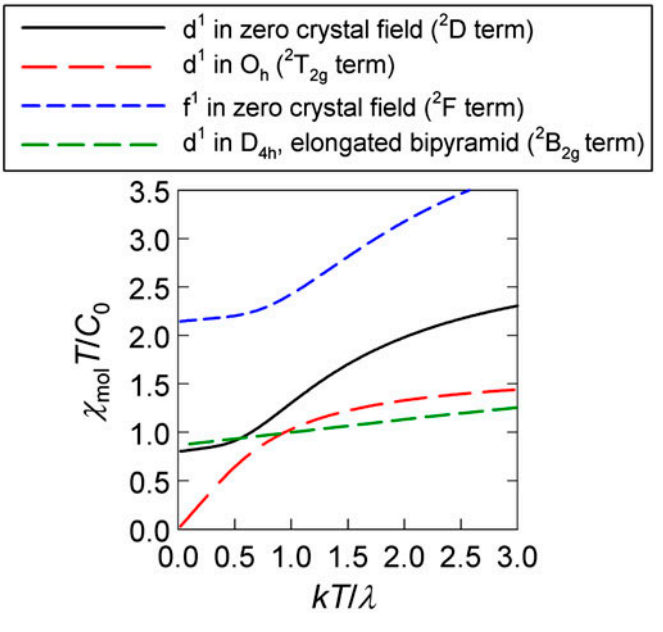

Figure 9. Modeling of the product function for mononuclear one-electron systems. The spin-orbit splitting parameter for Ce(III) ion is $\lambda/k = \xi/k = 920$ K.

The fitting procedure applied to the susceptibility and magnetization data-set gave $J/hc = -0.13\ \mathrm{cm}^{-1}$, $g = 2.455$, and $\chi_{\mathrm{TIM}} = 23 \times 10^{-9}\ \mathrm{m}^3\ \mathrm{M}^{-1}$; $R(\chi) = 0.040$ and $R(M) = 0.027$. The negative value of the exchange coupling constant arises from the ground state $S = 0$.

Then, the magnetic susceptibility on cooling should pass through a maximum at $|J|kT_{max} = 1.599$, so that $T_{max} = 0.12$ K and is not experimentally detected [37].

The fitted data of the effective magnetic moments follow a straight line; however, the experimental data show some curvature. Figure 9 brings the results of modeling of the dimensionless product function χT *versus* reduced temperature for a number of limiting cases: (i) ^2F term of the f^1 configuration in a free atom; (ii) ^2D term of the d^1 configuration in the free atom; (iii) $^2T_{2g}$ term of the d^1 configuration in the octahedral environment; and (iv) $^2B_{2g}$ term of the d^1 configuration in the geometry of an elongated tetragonal bipyramid (D_{4h}). None of these model systems are appropriate to the present case since we are dealing with nine-coordination of a d^1 system at low crystal-field symmetry; most close to this situation is the case (iv), where the orbital degeneracy is switched off by the low symmetry of the crystal field.

4. Conclusion

$\{[Gd_2(PDOA)_3(H_2O)_6]\cdot 2H_2O\}_n$ (**1**) and $\{[Ce_2(PDOA)_3(H_2O)_6]\cdot 2H_2O\}_n$ (**2**) were prepared using hydrothermal methods, which are commonly used for the preparation of new coordination compounds with Ln(III) [20, 25, 38, 39]. X-ray structure analyses corroborated the fact that both **1** and **2** contain ladder-like arrangements of the nine-coordinated Gd(III) and Ce(III) (the donor set is O_9), which are linked by short *syn-anti* carboxylate bridges and long bridges formed by PDOA. The phase identities of the single-crystal phases and those of the bulk samples were confirmed by powder X-ray diffractometry. Magnetic studies at temperatures down to 2 K revealed only very weak antiferromagnetic interactions between pairs of Ln(III) ions. Similar antiferromagnetic interactions in Gd(III) and Ce(III) complexes were already observed [40, 41].

Supplementary material

Crystallographic data for **1** and **2** have been deposited with the Cambridge Crystallographic Data Center, CCDC 974013 (**1**) and CCDC 974014 (**2**). Copies of the information may be obtained free of charge from The Director, CCDC, 12 Union Road, Cambridge, CB21EZ, UK (Fax: +44-1223-336033; E-mail: deposit@ccdc.cam.ac.uk or www: http://www.ccdc.cam.ac.uk).

Funding

This work was supported by the Slovak grants VEGA [grant number 1/0075/13], [grant number 1/0233/12], APVV-0132–11 and APVV-0014-11. Funding from the Ministry of Science and Innovation (Spain) under grants MAT2011–27233-C02–1 (with cofinancing from European Union Regional Development Funds) and CONSOLIDER 25200 and from the Diputación General de Aragón is gratefully acknowledged. This publication is the result of the Project KVARK – quality education and skills development for doctoral and postdoctoral students of P.J. Šafárik University in Košice, ITMS: 26110230084, supported by the Research & Development Operational Program funded by the ESF.

References

[1] Y.-J. Cui, Y.-F. Yue, G.-D. Qian, B.-L. Chen. *Chem. Rev.*, **112**, 1126 (2012).
[2] S. Mishra. *Coord. Chem. Rev.*, **252**, 1996 (2008).
[3] S.V. Eliseeva, J.-C.G. Bünzli. *Chem. Soc. Rev.*, **39**, 189 (2010).

[4] G.S. Kottas, M. Mehlstäubl, R. Fröhlich, L. De Cola. *Eur. J. Inorg. Chem.*, 3465 (2007).
[5] R. Sessoli, A.K. Powell. *Coord. Chem. Rev.*, **253**, 2328 (2009).
[6] D.N. Woodruff, R.E.P. Winpenny, R.A. Layfield. *Chem. Rev.*, **113**, 5110 (2013).
[7] H.-Y. Wang, C.-J. Zhang, C.-H. Zhang, Q. Tang, Y.-G. Chen. *J. Coord. Chem.*, **64**, 1481 (2011).
[8] J.-W. Moon, L.W. Yeary, A.J. Rondinone, C.J. Rawn, M.J. Kirkham, Y. Roh, L.J. Love, T.J. Phelps. *J. Magn. Magn. Mater.*, **313**, 283 (2007).
[9] Z.-G. Wang, J. Lu, C.-Y. Gao, C. Wang, J.-L. Tian, W. Gu, X. Liu, S.-P. Yan. *Inorg. Chem. Commun.*, **27**, 127 (2013).
[10] J.J. Baldoví, S. Cardona-Serra, J.M. Clemente-Juan, E. Coronado, A. Gaita-Arino, A. Palii. *Inorg. Chem.*, **51**, 12565 (2012).
[11] B. Benmerad, K. Aliouane, N. Rahahlia, A. Guehria-Laïdoudi, S. Dahaoui, C. Lecomte. *J. Rare Earths*, **31**, 85 (2013).
[12] X. Feng, X.-L. Ling, L. Liu, H.-L. Song, L.-Y. Wang, S.-W. Ng, B.-Y. Su. *Dalton Trans.*, 10292 (2013).
[13] J. Zhou, L. Du, Z.-Z. Li, Y.-F. Qiao, J. Liu, M.-R. Zhu, P. Chen, Y. Hu, Q.-H. Zhao. *Polyhedron*, **54**, 252 (2013).
[14] C.A. Black, J.S. Costa, W.-T. Fu, C. Massera, O. Roubeau, S.J. Teat, G. Aromí, P. Gamez, J. Reedijk. *Inorg. Chem.*, **48**, 1062 (2009).
[15] T.-L. Chen, X.-Y. Yu, X. Zhao, Y.-H. Luo, J.-J. Yang, H. Zhang, X. Chen. *Inorg. Chem. Commun.*, **23**, 74 (2012).
[16] J. Wang, W.-P. Wu, L. Lu, L.-K. Zou, B. Xie. *J. Chem. Res.*, **37**, 73 (2013).
[17] D.-Y. Ma, L. Qin, H.-F. Guo, J.-X. Lin, H.-C. Wei. *Synth. Met.*, **175**, 30 (2013).
[18] C.A.F. de Oliveira, F.F. da Silva, I. Malvestiti, V.R. dos S. Malta, J.D.L. Dutra, N.B. da Costa Jr., R.O. Freire, S. Alves Jr. *J. Mol. Struct.*, **1041**, 61 (2013).
[19] H.-H. Song, Y.-J. Li, Y. Song, Z.-G. Han, F. Yang. *J. Solid State Chem.*, **181**, 1017 (2008).
[20] T.Y. Zhu, K. Ikarashi, T. Ishigaki, K. Uematsu, K. Toda, H. Okawa, M. Sato. *Inorg. Chim. Acta*, **362**, 3407 (2009).
[21] C.-G. Wang, Y.-H. Xing, Z.-P. Li, J. Li, X.-Q. Zeng, M.-F. Ge, S.-Y. Niu. *J. Mol. Struct.*, **921**, 126 (2009).
[22] X. Li, Y.-Q. Li, X.-J. Zheng, H.-L. Sun. *Inorg. Chem. Commun.*, **11**, 779 (2008).
[23] X.-J. Zheng, L.-P. Jin, S. Gao, S.-Z. Lu. *Inorg. Chem. Commun.*, **8**, 72 (2005).
[24] Y. Jiang, X.-S. Wu, X. Li, J.-H. Song, Y.-Q. Zou. *J. Coord. Chem.*, **63**, 36 (2010).
[25] X. Li, C.-Y. Wang, X.-J. Zheng, Y.-Q. Zou. *J. Coord. Chem.*, **61**, 1127 (2008).
[26] Y.-G. Huang, F.-L. Jiang, M.-C. Hong. *Coord. Chem. Rev.*, **253**, 2814 (2009).
[27] X. Li, X.-S. Wu, H.-L. Sun, L.-J. Xu, G.-F. Zi. *Inorg. Chim. Acta*, **362**, 2837 (2009).
[28] P. Gawryszewska, Z. Ciunik. *J. Photochem. Photobiol. A: Chem.*, **202**, 1 (2009).
[29] R. Boča, M. Stolárová, L.R. Falvello, M. Tomás, J. Titiš, J. Černák. in preparation.
[30] G.M. Sheldrick. *SADABS* (Version 2.03), University of Göttingen, Germany (2001).
[31] Oxford Diffraction. *CrysAlis RED*, Version 1.171.32.19, Oxford Diffraction, Abingdon, release 28-02-2008 CrysAlis171.NET (2008).
[32] A. Altomare, G. Cascarano, C. Giacovazzo, A. Guagliardi. *J. Appl. Cryst.*, **26**, 343 (1993).
[33] G.M. Sheldrick. *Acta Crystallogr.*, **A64**, 112 (2008).
[34] K. Brandenburg, H. Putz. *Crystal Impact Diamond, Crystal and Molecular Structure Visualization*, GbR, Postfach 1251, D-53002 Bonn, Germany (2008).
[35] L. Cañadillas-Delgado, J. Pasán, O. Fabelo, M. Julve, F. Lloret, C. Ruiz-Pérez. *Polyhedron*, **52**, 321 (2013).
[36] R.-S. Zhou, J.-F. Song, Q.-F. Yang, X.-Y. Xu, J.-Q. Xu. *J. Mol. Struct.*, **877**, 115 (2008).
[37] R. Boča. *A Handbook of Magnetochemical Formulae*, Elsevier, Amsterdam (2012).
[38] Y.-C. Chang, Q. Shuai, Z.-C. Pei. *J. Coord. Chem.*, **66**, 3137 (2013).
[39] H.-L. Wen, W. Wen, D.-D. Li, C.-B. Liu, M. He. *J. Coord. Chem.*, **66**, 2623 (2013).
[40] C.-F. Qiao, Z.-Q. Xia, Q. Wei, C.-S. Zhou, G.-C. Zhang, S.-P. Chen, S.-L. Gao. *J. Coord. Chem.*, **66**, 1202 (2013).
[41] J.-Z. Gu, Z.-Q. Gao. *J. Chem. Crystallogr.*, **42**, 283 (2012).

Note added in Proof: The structure of the Ce compound $[Ce_2(PDOA)_3(H_2O)_6]\cdot 2H_2O$ was reported recently by Junk et al.: T. Behrsing, G.B. Deacon, P.C. Junk, B.W. Skelton, A.N. Sobolev, A.H. White, *Z. Anorg. Allg. Chem.* **639**, 41 (2013).